JOURNAL OF CATALYSIS 94, 501–507 (1985)

Partial Oxidation of Methane with Nitrous Oxide over V_2O_5–SiO_2 Catalyst

K. J. ZHEN, M. M. KHAN, C. H. MAK, K. B. LEWIS, AND G. A. SOMORJAI

Materials and Molecular Research Division, Lawrence Berkeley Laboratory; and Department of Chemistry, University of California, Berkeley, California 94720

Received November 9, 1984; revised March 15, 1985

The partial oxidation of methane to methanol and formaldehyde can be achieved selectively on silica-supported vanadium pentoxide catalysts in the temperature range 460–500°C in a reactant mixture of CH_4, N_2O, and H_2O at 1 atm total pressure. The selectivity to CH_3OH and HCHO can be 100% at 460°C at low conversions (~0.2%) and contact time (1.2 s), and decreases to produce more CO with increasing temperature, contact time, and conversion. The activation energies are 22 ± 2, 40 ± 4, and 47 ± 4 kcal/mole for the production of HCHO, CH_3OH, and CO, respectively. The rate equations are Rate (CH_3OH) $\sim (CH_4)^{1/2}(N_2O)^{1/2}(H_2O)^{1/2}$, Rate (HCHO) $\sim (CH_4)^{1/2}(N_2O)^{1/3}$, and Rate (CO) $\sim (CH_4)^{1/2}(N_2O)(H_2O)^{-1}$. The products form by parallel reaction paths which are different from the sequential oxidation mechanism of methane on molybdena and in a lower temperature range than on molybdenum oxide. © 1985 Academic Press, Inc.

INTRODUCTION

The partial catalytic oxidation of methane to methanol or to formaldehyde provides intriguing new opportunities for the production of liquid fuels and chemicals. Recent studies in our laboratory and elsewhere have shown that silica-supported molybdenum oxide appears to be a suitable catalyst for these processes (*1–3*). In the temperature range of 550–580°C and at 1 atm total reactant pressure methane can be oxidized selectively to CH_3OH and HCHO in the presence of N_2O and H_2O at low conversions (1–2%) and at low contact times. The fraction of formaldehyde increases with increasing contact time and its activation energy of formation is identical to that of CH_3OH at the higher temperatures. This indicates that formaldehyde is the product of a secondary reaction involving the further partial oxidation of methanol on the molybdena catalyst which is known to be an excellent catalyst for this reaction.

Our continued investigation uncovered that silica-supported vanadium pentoxide is also a good catalyst for the partial oxidation of methane and the purpose of this paper is to report our findings.[1] V_2O_5 produces methanol and formaldehyde selectively and at comparable conversions in the temperature range of 460–500°C. This is a significantly lower temperature range than that employed when using molybdenum oxide catalysts. The activation energies of HCHO and CH_3OH formation are different, 22 ± 2 and 40 ± 4 kcal/mole, respectively, indicating that their formation is by parallel reaction paths instead of the consecutive reaction sequence found on molybdena. The rates of CH_3OH, HCHO, and CO production are all ~half order in methane partial pressure and they also depend significantly on the partial pressures of N_2O and H_2O. The rate equations can be rationalized assuming the presence of a methoxy, $-OCH_3$, reaction intermediate that may hydrolyze to form methanol or may lose one or more hydrogen atoms to yield HCHO or CO.

---

[1] After this work was completed it was brought to our attention that M. Iwamoto has a Japanese patent (Jpn. Kokai Tokkyo Koho JP 5892630 CA 99: 157833r) on the partial oxidation of methane with N_2O over a 2% V_2O_5–SiO_2 catalyst using conditions similar to ours.

0021-9517/85 $3.00

Carbon dioxide is not detectable during the reaction.

EXPERIMENTAL

Materials. The catalyst, 2.0% V_2O_5–SiO_2, was prepared by impregnation from a basic solution of ammonium metavanadate at a pH of 10.5 and a subsequent drying followed by heating in air at 550°C. The support, Cab-O-Sil HS-5 fumed silica, had a reported surface area of 350 ± 25 m^2 g^{-1}. The finished catalyst was pressed and sifted to 30–60 mesh particles. The final surface area, as determined by BET measurement, was found to be 230 ± 10 m^2 g^{-1}. The active vanadium surface area was not determined, but it is well below the loading reported to be necessary for a monolayer coverage. The reactant gases, methane (99.9%), nitrous oxide (99.0%), oxygen (99.8%), and the carrier gas, helium (99.9%) were used as received.

Apparatus and methods. The fixed-bed reactor and the continuous flow manifold were the same as used in a study reported earlier (*1*). Reactant and carrier gases from the manifold and water vapor from a steam boiler were adjusted to the desired composition and passed through the catalyst bed at a total flow rate of 80 cm^3 min^{-1}. Typically, a molar composition of 0.15 CH_4, 0.30 N_2O, 0.40 H_2O, and 0.15 He at 1 atm total pressure and ~0.73 g (2 cm^3) catalyst was employed for most of the experiments. The entire reaction manifold was heated to 120°C to prevent condensation of water vapor. The analysis of the gas mixture before and after reaction was carried out gas chromatographically using a thermal conductivity and a flame ionization detector. The reaction temperature was controlled and monitored with a probe thermocouple embedded in the catalyst bed. The reaction was initiated by flowing 80 cm^3 min^{-1} of the reaction mixture of a desired composition through the catalyst bed preset to the reaction temperature, usually between 460 and 500°C. One to two hours was allowed for the system to reach a steady state and be ready for sample analysis.

Analytical procedure. An in-line gas chromatograph, equipped with a 10-port sampling valve, a flame ionization (FI) detector, a thermal conductivity (TC) detector, and two analytical columns were used for alternate injections into the two columns, one leading to the TC detector and the other to the FI detector. The pre- and postreaction samplings were made possible by incorporating a six-port switching valve into the reaction manifold. Separation and detection of (N_2 + O_2), CO, CO_2, CH_4, N_2O, and H_2O were accomplished with a Carbosieve S-II (Supelco) column and a TC detector. For CH_3OH, HCHO, CH_4, and higher hydrocarbons, a Porapak-QS column and a flame ionization detector at a sensitivity of 12 pAFS were used. For quantitative analysis the measured peak areas were corrected for the molar response factors of the various components as reported by Dietz (*4*).

The products, HCHO and CH_3OH, were collected by stripping the exit gas stream in a cold trap maintained at −5°C. Since there

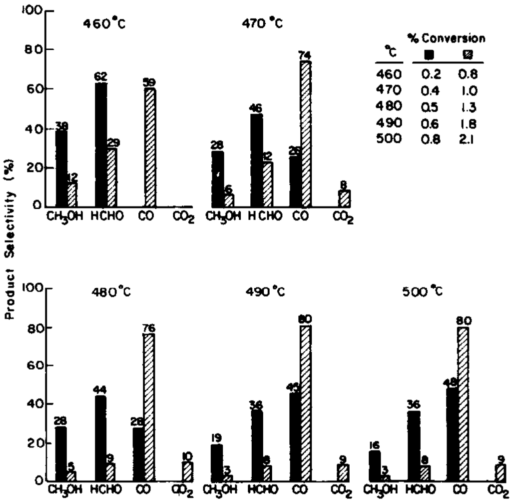

FIG. 1. Effects of temperature are contact time on conversion and product distribution. Solid bars: 1.2-s contact time; hatched bars: 4.6-s contact time. Composition (mole%): CH_4, 15; N_2O, 30; H_2O, 40; He, 13; and O_2, 2.

was a considerable amount of steam in the reaction mixture, the condensate was trapped in the form of an aqueous solution of a mixture of HCHO and CH_3OH with better than 99% efficiency. The analysis of the condensate was carried out gas chromatographically as described in a previous paper (*1*) and the rates of formation of CH_3OH and HCHO were calculated on the basis of the weight of the condensate collected over a timed interval. The rate of formation of CO was calculated as the product of the flux and the mole fraction of CO as determined by the GC analysis of the exit gas stream.

The reported rate data are based on the assumption of a 100% dispersion of vanadium over the support, since at a 2% loading, vanadium is known to have submonolayer coverage over a support of similar surface area (*5*).

RESULTS

Yield and product distribution. Figure 1 summarizes the effects of temperature and contact time on the overall conversion of methane and the relative product distribution of CH_3OH, HCHO, and CO expressed as a mole percentage of the total. At a contact time of 1.2 s, the overall conversion varied from 0.2% at 460°C to 0.8% at 500°C. Both CH_3OH and HCHO selectivities dropped and CO selectivity increased with the increase in temperature. For example, at 460°C CH_3OH and HCHO formed with selectivities of 38 and 62%, respectively. These decreased to 16 and 36%, respectively, at 500°C, while the CO selectivity increased from 0 to 48% over the same temperature range. No CO_2 formation was observed at a contact time of 1.2 s over this temperature range. Increased contact time had a more adverse effect on the product selectivities toward CH_3OH and HCHO. Higher temperature and contact time resulted in the formation of increased amounts of CO and CO_2 at the expense of CH_3OH and HCHO. As shown in the hatched bar graphs in Fig. 1, the formation of CH_3OH and HCHO were marked with substantially lower selectivities of 12 and 29%, respectively, at 460°C when the contact time was increased to 4.6 s. At higher temperatures, especially in the range of 480–500°C, CO was the major product, with an 80% selectivity. Moreover, this increase in contact time to 4.6 s even led to the formation of a small amount of CO_2, a product which was not detected under the flow conditions of a 1.2-s contact time. It is also to be noted from Fig. 1 that the overall conversion of CH_4 more than doubled with the increase in contact time from 1.2 to 4.6 s. At 460°C, for example, the conversion increased from 0.2 to 0.8% with this increase in contact time but the selectivity of CH_3OH and HCHO dropped from 38 and 62% to 12 and 29%, respectively, with the increase in selectivity of CO from 0 to 59%.

Temperatures below 460°C were too low for the detection of CH_3OH and HCHO with any reliability. Above 500°C CO and CO_2 were the predominant products and therefore this temperature region was not investigated.

Experiments were initially performed using O_2 as the oxidant. At 500°C, 1.2-s contact time with oxygen alone as the oxidant gives greater than 80% selectivity for CO and CO_2 with 0.7% conversion. Under the same conditions but with N_2O as the oxidant 100% selectivity for CH_3OH and HCHO is obtained with 0.1% conversion. However, a small quantity (2%) of O_2 added to the reaction mixture with N_2O as the oxidant gives 48, 36, and 16% selectivity for CO, HCHO, and CH_3OH, respectively, with 1.0% conversion. Due to this enhanced conversion much of the work presented in this paper was performed with 2% O_2 in the reaction mixture.

Reaction rates and kinetic parameters. The turnover rates of CH_3OH, HCHO, and CO observed over the temperature range of 460 to 500°C and contact times of 1.2 and 4.6 s are presented in Table 1. At a contact time of 1.2 s and an 80-cm^3 min^{-1} flow of $0.15\,CH_4 + 0.30\,N_2O + 0.40\,H_2O + 0.13\,He$

TABLE 1

Conversion and Turnover Rates at Various Temperatures and Contact Times

Temp (°C)	Contact time (s)	Turnover rate × 10^4 (molec. s^{-1} · $atom^{-1}$)			Total conv. percentage
		CH_3OH	HCHO	CO	
460	1.2	0.38	0.63	0	0.2
	4.6	0.12	0.228	0.38	0.8
470	1.2	0.46	0.88	0.44	0.4
	4.6	0.084	0.144	0.66	1.0
480	1.2	0.81	1.0	0.56	0.5
	4.6	0.079	0.144	0.86	1.3
490	1.2	0.97	1.2	1.1	0.6
	4.6	0.078	0.178	1.23	1.8
500	1.2	1.21	1.5	1.40	0.8
	4.6	0.081	0.21	1.34	2.1

Note. Reactant composition: 0.15 CH_4 + 0.30 N_2O + 0.40 H_2O + 0.13 He + 0.02 O_2. Total flow: 80 cm^3 min^{-1}.

+ 0.02 O_2 through the catalyst bed at 490°C, CH_3OH, HCHO, and CO were formed at turnover rates of 1×10^{-4}, 1.2×10^{-4}, and 1.1×10^{-4} molec. s^{-1} · $atom^{-1}$, respectively, with an overall yield of 0.6%. However, at a higher contact time of 4.6 s the net rates of formation of CH_3OH and HCHO dropped to 0.08×10^{-4} and 0.18×10^{-4}, respectively, whereas, that of CO increased to 1.2×10^{-4} with an overall yield of 1.8% at the same conditions of reactant composition and temperature. This increased rate of CO formation with concomitant decreases in CH_3OH and HCHO formations as a function of increased contact time was reflected in the product distribution data discussed in the previous section.

As shown in Fig. 2, the temperature dependence of the rates of formation of CH_3OH, HCHO, and CO were found to give an Arrhenius fit within the limits of experimental uncertainty over the entire temperature range of 460–500°C. The activation energies were 22 ± 2, 40 ± 4, and 47 ± 4 kcal/mole for the formation of HCHO, CH_3OH, and CO, respectively. Due to the scatter in the data, the latter two values are probably not significantly distinct.

The logarithmic plots of the various rates vs the mole percentage of the reactant of interest were obtained as shown in Figs. 3 through 6, with the relevant composition data specified therein.

The kinetic order at 500°C, as determined

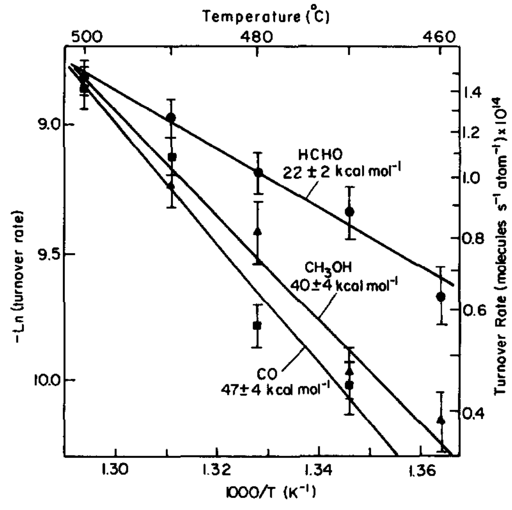

FIG. 2. Arrhenius plots for formation of CH_3OH, HCHO, and CO. Reactant gas: 80-cm^3 min^{-1} flow of 0.15 CH_4 + 0.30 N_2O + 0.40 H_2O + 0.15 He, contact time of 1.2 s.

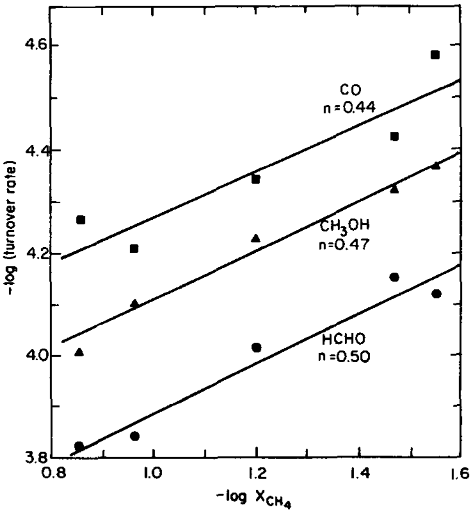

FIG. 3. CH_4 pressure dependence of turnover rates at 500°C. Composition (mole%): CH_4, 2.8 to 14; N_2O, 22; H_2O, 40; O_2, 1.6; and balance He.

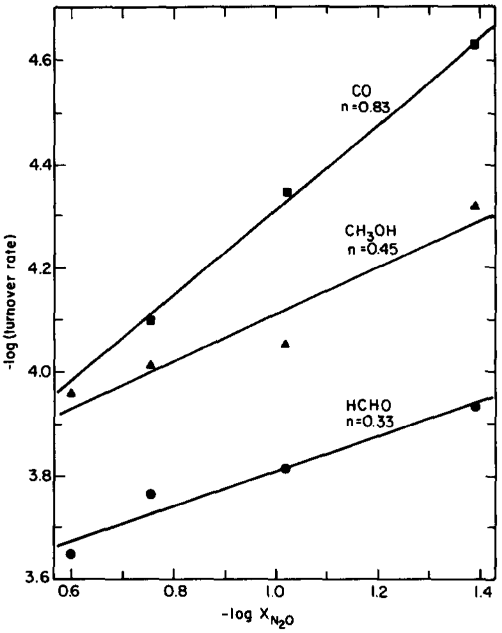

FIG. 4. N_2O pressure dependence of turnover rates at 500°C. Composition (mole%): N_2O, 4 to 25; CH_4, 14; H_2O, 40; O_2, 1.6; and balance He.

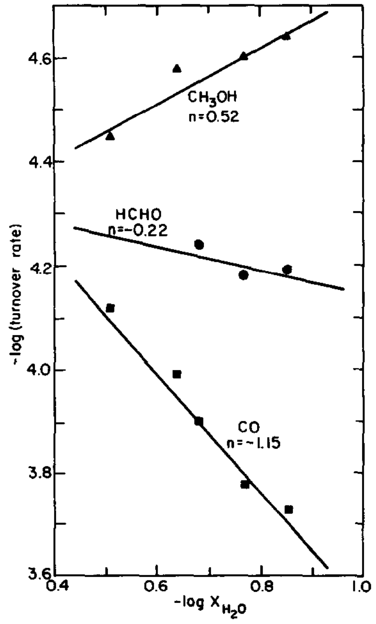

FIG. 5. H_2O pressure dependence of turnover rates at 500°C. Composition (mole%): H_2O, 14 to 31; CH_4, 4; N_2O, 28; O_2, 1.6; and balance He.

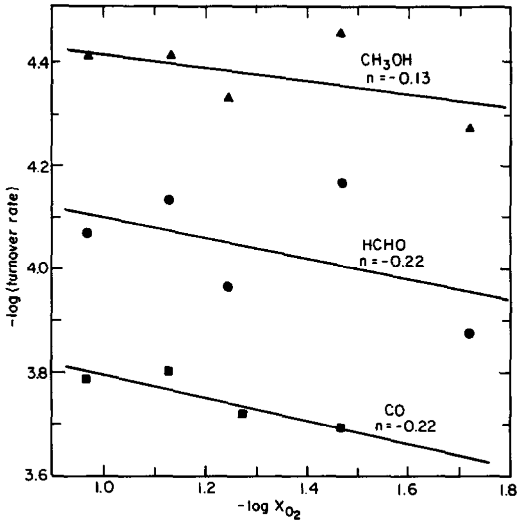

FIG. 6. O_2 pressure dependence of turnover rates at 500°C. Composition (mole%): O_2, 2 to 11; CH_4, 13; N_2O, 10; H_2O, 37; and balance He.

from these figures revealed the following rate laws.

$$\text{Rate }(CH_3OH) \propto [CH_4]^{1/2}[N_2O]^{1/2}[H_2O]^{1/2}$$

$$\text{Rate }(HCHO) \propto [CH_4]^{1/2}[N_2O]^{1/3}$$

$$\text{Rate }(CO) \propto [CH_4]^{1/2}[N_2O]^{1}[H_2O]^{-1}$$

The order with respect to CH_4 was one-half for the rates of formation of all three products over a CH_4 mole% range of 3 to 14. At lower concentrations the rate was too low to be measured accurately and at higher concentrations deactivation due to excessive coking was observed. For N_2O pressure dependence a N_2O mole% range of 4 to 25 was found suitable for the measurement. CH_3OH, HCHO, and CO formed with, respectively, one-half, one-third, and first-order kinetics with respect to N_2O. The steam pressure dependence was, respectively, one-half, zero, and negative first. For the measurement of kinetic order with respect to H_2O, a much lower concentration of methane of 4% instead of the usual 13–14% was necessary to prevent cracking of CH_4 at the lower range of steam pressure. The slight negative dependence on the oxygen partial pressure is not thought to be significant due to the large scatter of the data points. Therefore we assume that it is zero within the experimental error.

DISCUSSION

Conversion and product selectivity. It is worthwhile to draw a comparison between this and the previously reported works on MoO_x–SiO_2 catalysts (*1–3*). First, the working range for vanadium pentoxide (450–500°C) is comparatively lower and narrower than observed in the case of MoO_x–SiO_2 catalyst, which was 480–590°C under similar conditions at reactant composition and contact time. Compared to MoO_x–SiO_2, V_2O_5–SiO_2 catalyst was found to be more active for CH_3OH formation at the overlapping temperatures of the above two ranges. For instance, at 490°C, the turnover rate for CH_3OH formation on MoO_3–SiO_2, 0.50×10^{-4} molec. $\text{site}^{-1} \cdot \text{s}^{-1}$, was substantially lower than was observed on V_2O_5–SiO_2, which was 0.97×10^{-4} molec. $\text{site}^{-1} \cdot \text{s}^{-1}$. The total conversion was also more favorable on V_2O_5–SiO_2, 0.10% at 2.3-s contact time on MoO_3–SiO_2 as compared with 0.6% at 1.2-s contact time on V_2O_5–SiO_2. It appears that V_2O_5–SiO_2 is a considerably stronger oxidizing catalyst than MoO_3–SiO_2, which has the favorable consequence of lower operating temperature. However, V_2O_5–SiO_2 has an unfavorable product selectivity toward CH_3OH.

Kinetics and mechanisms. A comparison of the rate laws of various product formations and activation energies is provided in Table 2. In our previous report on MoO_3–SiO_2 (*1*), the two E_a values for HCHO were ascribed to two different mechanisms, a low-temperature path leading to the HCHO formation simultaneously with CH_3OH from the same intermediate with an activation energy of 82 ± 2 kcal/mole, and a lower-activation-energy, high-temperature process involving further oxidation of CH_3OH. For the methane oxidation on V_2O_5–SiO_2, however, the mechanism seems to be entirely different. Even though the E_a for CH_3OH formation is very similar (40 kcal/mole) to that on MoO_3, the activation energy for HCHO is substantially lower. Furthermore, there is no evidence for any consecutive oxidation of CH_3OH leading to HCHO or CO.

TABLE 2

Rate Laws and Activation Energies

Product	Rate law	E_a (kcal/mole)
	V_2O_5–SiO_2 catalyst	
CH_3OH	$[CH_4]^{1/2}[H_2O]^{1/2}[N_2O]^{1/2}$	40 ± 4
HCHO	$[CH_4]^{1/2}[H_2O]^{0}[N_2O]^{1/3}$	22 ± 2
CO	$[CH_4]^{1/2}[H_2O]^{-1}[N_2O]^{1}$	47 ± 4
	MoO_3–SiO_2 catalyst[a]	
CH_3OH	$[CH_4]^{1}[H_2O]^{1}[N_2O]^{0}$	41 ± 2
HCHO	$[CH_4]^{0}[H_2O]^{0}[N_2O]^{0}$	82 ± 2 (low temp), 40 ± 2 (high temp)
CO	Not available	Not available

[a] Khan and Somorjai (Ref. (*1*)).

Although we cannot rule out mechanisms with branched or sequential reactions, the simplest mechanism that fits our kinetic data is one involving parallel reaction paths for the formation of CH_3OH, HCHO, and CO on the V_2O_5–SiO_2 catalysts.

Speculation on the reaction mechanisms. The chemisorption of methane which occurs with a very low reaction probability produces a methoxy group, CH_3O–, and a hydroxyl group. Hydrolysis of the methoxy group by water yields methanol and another hydroxyl group on the vanadium oxide surface. However, CH_3O can also undergo sequential loss of hydrogen atoms to produce HCHO and CO molecules which then desorb. Dehydroxylation of the oxide surface can occur by oxidative elimination with the help of dissociatively chemisorbed N_2O. The reaction is also likely to be structure sensitive as there are several different oxygen sites on the different vanadium oxide crystal surfaces. These are likely to show different activity toward the production of CH_3O– groups. It is possible that twin vanadium–oxygen units are required for the dissociative chemisorption of methane which would make this reaction even more structure sensitive.

Since the formation of CH_3OH, HCHO, and CO proceeds by parallel reactions it appears possible to block some of the reaction paths by suitable additives thereby increasing the selectivity.

In addition, the selectivity and reaction yield could be further enhanced by increasing the total pressure of the reactants. In this study the total pressure was constant at 1 atm. Further studies are planned to investigate the effect of increased total pressure.

ACKNOWLEDGMENTS

This work was supported by the Director, Office of Energy Research, Office of Basic Energy Sciences, and the Divisions of Materials Science and Chemical Sciences of the U.S. Department of Energy under Contract DE-AC03-76SF00098.

REFERENCES

1. Khan, M. M., and Somorjai, G. A., *J. Catal.* **91,** 263 (1985).
2. Liu, R.-S., Iwamoto, M., and Lunsford, J. H., *J. Chem. Soc. Chem. Commun.,* 78 (1982).
3. Lin, H. F., Liu, R.-S., Liew, K. Y., Johnson, R. E., and Lunsford, J. H., *J. Amer. Chem. Soc.* **106,** 4117 (1984).
4. Dietz, W. A., *J. Gas Chromatogr.* **5,** 68 (1967).
5. Iwamoto, M., Mori, K., Miyamoto, A., and Murakami, Y., *J. Phys. Chem.* **87,** 761 (1983).